Colloquia: LaThuile12

Latest top physics results at ATLAS

L. Mijović(*) on behalf of the ATLAS Collaboration

CEA-Saclay, IRFU/SPP - bât. 141, 91191 Gif sur Yvette Cedex, France

Summary. — Recent top-physics results obtained at ATLAS using the LHC data collected during 2011 are reviewed. For the top and antitop pair production process, measurements of the cross section and the top quark mass are summarized and the measurements yielding the most precise results are discussed. Results of other recent measurements of top quark properties in top and antitop pair production production events are summarized. Then the searches for the new physics predicting top quark production mechanisms other than Standard Model ones or final-state signatures similar to the top production processes signatures are reviewed. Finally measurements in the single-top production processes are reviewed.

PACS `14.65.Ha` – Top quarks.

1. – Introduction

In 2011, the LHC delivered an integrated luminosity of $\mathcal{L}_{\text{int}} = 5.6\,\text{fb}^{-1}$ of pp collisions at $7\,\text{TeV}$ centre-of-mass energy to the ATLAS [1] experiment. The data fulfilling all quality requirements of top quark production analyses corresponds to the integrated luminosity of $\mathcal{L}_{\text{int}} = 4.7\,\text{fb}^{-1}$. The top physics results obtained to date with the 2011 data are presented in this contribution(^{1}). At the LHC top quarks are predominantly produced via the strong-interaction processes resulting in pair production of top and antitop ($t\bar{t}$ production). The pair production cross section is approximately twice as large as the total cross section of the weak-interaction production leading to single-top-quark final states. The latter include the exchange of a virtual W boson in the t-channel or in the s-channel, and the associated production of a top quark and an on-shell W boson (Wt-channel production). The top quark is expected to decay to a W boson and a b quark with a branching ratio B_r close to 1. For the $t\bar{t}$ production the decay channels are classified depending on the W boson decays as follows: in dileptonic, single lepton and fully hadronic decay channel both, one and none of the W bosons decays to leptons.

The top quark production event selection consists of event cleaning, trigger requirements, requirements on the multiplicities of the final-state object and event properties requirements that are expected to enhance the signal (S) over background (B) ratio. The event cleaning includes the detector and data quality requirements, the presence of at

---

(*) E-mail: `liza.mijovic@cern.ch`
(^{1}) All public ATLAS top quark physics results are available at [2].

least one good primary vertex candidate [3] and the absence of jets failing quality criteria [4] as well as requirements aimed at cosmic background rejection. The trigger, object and event properties requirements are analysis specific and are detailed *e.g.* in refs. [5-7] for dileptonic, single lepton and fully hadronic $t\bar{t}$ decay channel analyses and in refs. [8-10] for single top t-, Wt- and s- production channel analyses. Typical kinematic requirements used for e (μ, jet) are ($|\eta| < 2.5$) and $E_{\mathrm{T}} > 25\,\mathrm{GeV}$ ($p_{\mathrm{T}} > 20\,\mathrm{GeV}$) or higher, where η, E_{T} and p_{T} denote the pseudorapidity(^{2}), transverse energy and momentum, respectively. Jets are reconstructed using the anti-k_t algorithm [11] with a radius parameter of 0.4. Clusters of adjacent calorimeter cells [12] are used as clustering inputs. The missing transverse momentum ($E_{\mathrm{T}}^{\mathrm{miss}}$) is calculated using clusters of adjacent calorimeter cells and corrected for the presence of e, μ and jets [13]. The identification of jets originating from b quarks is performed using a discriminant obtained from one or combination of more b tagging algorithms. The taggers rely on impact parameters of the track within the jet (IP3D), properties of the vertices reconstructed within the jet (SV1) or topology of b and c hadron decays (JetFitter) [14]. The tagger working points are typically chosen such that the tagging efficiency of $\sim 60\%$–70% and the light jet rejection of ~ 500 are achieved.

For each of the top quark production processes a number of Monte Carlo (MC) generators and setups is used for the baseline MC prediction and to assess the modeling systematics. For the $t\bar{t}$ and s- and Wt-channel single-top events the baseline samples are generated using MC@NLO [15] generator interfaced to HERWIG [16] and JIMMY [17]. For t-channel the ACERMC generator [18] interfaced to PYTHIA (v6) [19] is used. Supervising generators parameters are set according to tunes including ATLAS data [20, 21]. Samples generated with POWHEG-hvq [22], interfaced with PYTHIA as well as HERWIG and JIMMY, ALPGEN [23], interfaced with HERWIG and JIMMY, and SHERPA [24] generators are used for modeling systematics. Apart from generator to generator comparisons the modeling systematics is also addressed by using dedicated samples with PYTHIA generator parameter variations. The bulk of background samples is generated with ALPGEN interfaced to HERWIG and JIMMY generators. Generated events are processed through the simulation of the ATLAS detector that relies on GEANT4 simulation toolkit [25]. The reconstruction of simulated samples is performed using the same software release as for the data. Pile-up is simulated using minimum bias events generated with PYTHIA (v6) generator. Signal Monte Carlo samples are normalized such that inclusive cross sections correspond to the recent theoretical predictions. For analyses discussed in this contribution the $t\bar{t}$ cross section is normalized to the approximate next-to-next-to-leading–order prediction value of $164.6 + 11.5 - 15.8\,\mathrm{pb}$, obtained using the HATHOR tool [26] and CTEQ6.6 NLO parton distribution functions (PDF) set [27]. Single top production cross sections are normalized to the approximate next-to-next-to-leading–order prediction values of $64.6 + 2.7 - 2.0\,\mathrm{pb}$, $4.6 \pm 0.2\,\mathrm{pb}$ and $15.7 \pm 1.1\,\mathrm{pb}$ for the t, s and Wt production channels, respectively [28]. Reference single-top cross section values are obtained using MSTW2008 NNLO PDF set [29]. For both $t\bar{t}$ and single top production the uncertainties are obtained by linear addition of PDF and scale uncertainties. The cross sections are evaluated at the top quark mass of $m_t = 172.5\,\mathrm{GeV}$ that is used for simulated samples.

(^{2}) ATLAS uses a right-handed coordinate system with its origin at the nominal interaction point (IP) in the centre of the detector and the z-axis along the beam pipe. The x-axis points from the IP to the centre of the LHC ring, and the y axis points upward. Cylindrical coordinates (r, ϕ) are used in the transverse plane, ϕ being the azimuthal angle around the beam pipe. The pseudorapidity is defined in terms of the polar angle θ as $\eta = -\ln\tan(\theta/2)$.
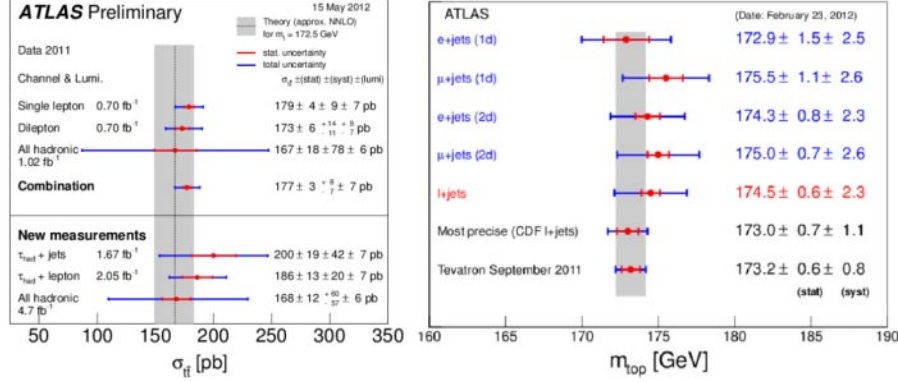
Fig. 1. – Left: summary of ATLAS measurements of the $t\bar{t}$ production cross section compared to the theoretical expectation [2]. Right: measurements on the top quark mass from the individual ATLAS analyses and the combined result from the 2d analysis described in the text. The results are compared to the results of the Tevatron experiments [30].

2. – $t\bar{t}$ production measurements

Measurements in $t\bar{t}$ production processes obtained to date with the data collected in 2011 are summarized in the following.

Measurements of $t\bar{t}$ production cross section enable precision tests of perturbative QCD predictions. Cross section measurements are also of importance for new physics searches, since many new physics models predict the existence of additional production mechanisms that result in enhancements of the $t\bar{t}$ production cross section with respect to the Standard Model prediction. The knowledge of $t\bar{t}$ production rates in various kinematic regimes is needed for many new physics searches for which $t\bar{t}$ production represents an important background. The cross section measurements at ATLAS with the data collected in 2011 are summarized and compared to the theoretical expectation in fig. 1 (left). The total uncertainty of the combined result is comparably small to the state of the art theory calculations (sect. **1**) and the systematics uncertainty exceeds the statistical uncertainty.

The ATLAS single most precise cross section measurement is obtained in the single-lepton (e or μ) decay channel [6] using $\mathcal{L}_{\text{int}} = 0.7\,\text{fb}^{-1}$ of collected data. Apart from the lepton requirement, events are requested to contain large $E_{\text{T}}^{\text{miss}}$ and at least three high p_{T} jets. The method for signal and background separation exploits differences in distributions of the following kinematic variables: lepton η, leading jet p_{T} and event shape variables aplanarity and $H_{\text{T},3\text{p}}$(^{3}). These observables are used as inputs to a likelihood discriminant. The analysis is performed in six channels corresponding to different lepton flavor (e or μ) and jet multiplicity (3, 4 and ≥ 5 jets). Signal and background templates are constructed for each of the channels and the $t\bar{t}$ cross section is extracted from a simultaneous fit of the templates to the the data:

$$(1) \qquad\qquad \sigma_{t\bar{t}} = 179.0 \pm 4(\text{stat.}) \pm 9(\text{syst.}) \pm 7(\text{lumi.})\,\text{pb}.$$

(^{3}) $H_{\text{T},3\text{p}}$ corresponds to the transverse momentum of all but the two leading jets, normalized to the sum of absolute values of all longitudinal momenta in the event.
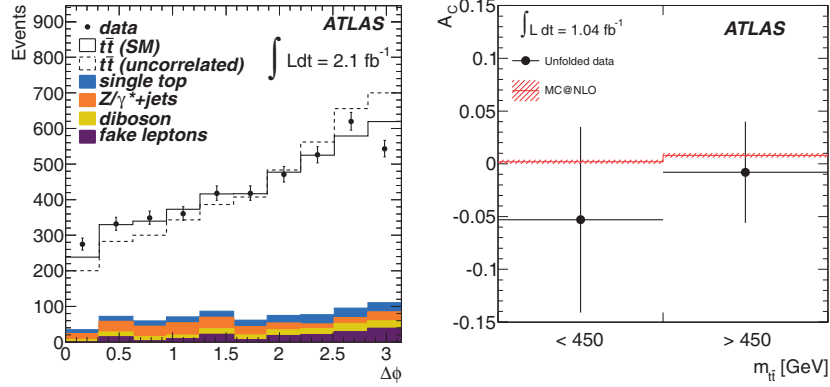
Fig. 2. – Left: lepton $\Delta\varphi$ distribution used for the measurement of the spin correlation in $t\bar{t}$ production [31]. Right: $t\bar{t}$ charge asymmetry values in two $t\bar{t}$ invariant-mass bins, unfolded and compared to the theoretical SM prediction [32].

Dominant sources of systematic uncertainty are the choice of the signal MC generator, followed by the jet energy scale and initial and final state radiation modeling uncertainties.

The top quark mass m_t is a fundamental parameter of the Standard Model (SM). It can be used to derive constraints on the masses of the Higgs boson and of heavy particles predicted by SM extensions. Measurements of m_t performed at ATLAS with the data collected in 2011 are summarized and compared to Tevatron experiments results in fig. 1 (right). The most precise measurement is obtained in the single-lepton (e or μ) $t\bar{t}$ channel [30] using data corresponding to the integrated luminosity of $\mathcal{L}_{\text{int}} = 1.04\,\text{fb}^{-1}$. The m_t is extracted using a two-dimensional template method (2d analysis). The two fitted quantities are the m_t and a global (averaged over η and p_{T}) jet energy scale factor (JSF). The main observables from which the m_t and JSF are extracted are the selected jet pair and jet triplet invariant masses. These serve as estimators of the reconstructed W boson and reconstructed m_t. The combined value of e and μ channel results is,

$$(2) \qquad m_t = 174.5 \pm 0.6(\text{stat.}) \pm 2.3(\text{syst.})\,\text{GeV}.$$

While the statistical uncertainty of the ATLAS and Tevatron measurements are comparable, a reduction of the systematics uncertainty claimed by ATLAS is needed in order to reach the Tevatron measurements precision. The largest sources of systematics are the relative b-jet to light jet energy scale, followed by the light quark jet energy scale and the modeling of the initial and final state radiation. These sources account for $\sim 85\%$ of the systematic uncertainty.

Spin correlation in $t\bar{t}$ production has been measured with the data corresponding to $\mathcal{L}_{\text{int}} = 2.05\,\text{fb}^{-1}$ in dileptonic (e or μ) decay channel [31]. Due to its short life-time the top quark is expected to decay before hadronising. The spin correlation of t and $\bar{t}$ is transferred to decay products and can be inferred from their respective angular distributions. The lepton $\Delta\varphi$ distribution shown in fig. 2 (left) is found to be a sensitive observable. The distribution measured in the data is compared to the theoretical predictions obtained in the cases of t and $\bar{t}$ spin correlations as predicted by the SM and the uncorrelated t and $\bar{t}$ spin hypothesis. Using templates produced from samples with and without spin correlations a fraction of SM-like events is extracted and found to be consistent with 1.0. The hypothesis of zero spin correlation is excluded at 5.1 standard deviations.

TABLE I. – *Summary of 95% confidence level (CL) limits obtained in searches for the pair-produced heavy quarks, same-sign top production and resonances decaying to top quarks at AT-LAS with the data collected in* 2011.

Process	Channel	$\mathcal{L}_{\text{int}}$ [fb^{-1}]	Excl. limits	Ref.
		pair-produced heavy quarks $Q\overline{Q}$		
$Q\overline{Q} \to W^+qW^-\bar{q}$ $(q = u, d, c, s, b)$	dilepton	1.04	$m_Q < 350\,\text{GeV}$	[39]
$Q\overline{Q} \to W^+bW^-\bar{b}$	single lepton	1.04	$m_Q < 404\,\text{GeV}$	[40]
$Q\overline{Q} \to W^+tW^-\bar{t}$	single lepton	1.04	$m_Q < 480\,\text{GeV}$	[42]
$Q\overline{Q} \to W^+tW^-\bar{t}$	dilepton	1.04	$m_Q < 450\,\text{GeV}$	[41]
$Q\overline{Q} \to t\bar{t} + E_{\text{T}}^{\text{miss}}$	single lepton	1.04	$m_Q < 420\,\text{GeV}$, $m_{A_0} < 140\,\text{GeV}$	[43]
		Resonances decaying to top final states		
tt	$\mu^+\mu^+, \mu^-\mu^-$	1.6	$\sigma'_Z = 3.7 - 2.2\,\text{pb}$ for $m_{Z'} = 0.1 - \gg 1\,\text{TeV}$	[44]
tt	$l^+l^+, l^-l^-, l = e, \mu$	1.04	$\sigma'_Z = 2.0 - 1.4\,\text{pb}$ for $m_{Z'} = 0.1 - 0.2\,\text{TeV}$	[41]
$t\bar{t}$	di- & single lept.	2.05	$500 < m_{Z'} < 880\,\text{GeV}$, $500 < m_{g_{KK}} < 1130\,\text{GeV}$	[45]
tb	$l\nu bb$	1.04	$m_{W'_R} < 1.13\,\text{TeV}$	[46]

The charge asymmetry A_c measurement has been performed with $\mathcal{L}_{\text{int}} = 1.04\,\text{fb}^{-1}$ in the single-lepton (e or μ) channel [32]. LHC A_c measurement are particularly interesting due to the deviations from the SM predictions recently reported for forward-backward asymmetry by the Tevatron experiments [33]. Results of the measurements done at ATLAS to date yield results consistent with SM predictions, as shown in fig. 2 (right).

Further top quark property measurements in $t\bar{t}$ events include the measurement of W polarization [34], top quark charge [35] and searches for flavor-changing neutral-current (FCNC) decays of the top quark [36]. In all cases the results are consistent with the SM expectations. The measurements of the $t\bar{t}$ production in association with jets [37] and photons [38] have also been performed.

3. – New particle searches in top(-like) production

A number of new particle searches have been performed in top(-like) production with the data collected in 2011. These include searches for pair-produced heavy quarks, same-sign top production and resonances decaying to top quarks. In these processes final-state signatures are similar to top quark production processes or top quarks are produced. The results are summarized in table I(^{4}). In all cases no excess over SM expectations has

(^{4}) The following labels are used in the table: A_0 denotes a stable, neutral weakly interacting particle, Z' denotes a narrow resonance, g_{KK} denotes a Kaluza-Klein gluon excitation in the Randall-Sundrum model and W'_R denotes a right-handed charged heavy gauge boson.

TABLE II. – *Summary of single-top cross section measurements at ATLAS.*

Channel	$\mathcal{L}_{\text{int}}$ [fb^{-1}]	Cross section [pb]	SM prediction [pb]	Ref.
t	1.04	83 ± 4(stat.)$ + 20 - 19$(syst.)	64.57 +2.7 -2.0	[8]
Wt	2.05	16.8 ± 2.9(stat.)± 4.9(syst.)	15.7 ± 1.1	[9]
s	0.70	$< 26.5(20.5)$ obs.(exp.) @ 95% CL	4.6 ± 0.2	[10]

been observed, which enables setting limits on new particle properties and new physics processes. Searches for pair-produced heavy quarks ($Q\overline{Q}$) are a direct tests of the fourth-generation quark existence. In the scenarios summarized in the table the heavy-quark mass m_Q exceeds the mass of the top quark and the $t\bar{t}$ production is the main background process. The limits quoted for refs. [39, 40] apply to heavy up- and down-type quark pair production as well as exotic quark pair production decaying to the final state used in the analysis. Many of new physics models predict the existence of resonances decaying to top quarks. The searches for same sign top production, $t\bar{t}$ and tb resonances summarized in the table enable setting more stringent limits on the resonance masses than the existing limits from Tevatron experiments. In ref. [41] the limits are also placed on models that could explain the larger than expected forward-backward asymmetry in $t\bar{t}$ production observed at Tevatron.

4. – Single-top production results

The single-top-quark production proceeds via the weak interactions. With respect to the $t\bar{t}$ production it provides additional means to probe tWb vertex. Single-top production is a sensitive probe of a number of new physics models [47]. It can also be used for direct measurements of the CKM matrix element $|V_{tb}|$. Hence, despite lower production rates and more challenging signal to background separation with respect to the $t\bar{t}$ production, a number of single-top production measurements have been performed ATLAS in 2011. The cross section measurements have been performed in the t, Wt and s channels. The measured values and their associated statistical and systematic (stat., syst.) uncertainties or upper observed and expected (obs.(exp.)) 95% CL limits are reported in table II.

In the t-channel measurement [8] the final states with one lepton (e, μ), $E_{\text{T}}^{\text{miss}}$, and two or three jets, exactly one of them identified as originating from a b quark, are selected. The multijet background and the normalization of the background coming from the W production in association with jets are derived from the data. Theoretical predictions are used for the $t\bar{t}$ backgrounds and other smaller background contribution processes. The cross section is measured by fitting the distribution of a multivariate discriminant constructed with a neural network (NN). The estimator of the invariant top mass, obtained from the b tagged jet, the charged lepton, and the neutrino is the NN input variable with the highest discrimination power. The NN output is shown in fig. 3 (left). The extracted cross section reported in table II is in good agreement with the SM prediction. Dominant sources of systematic uncertainty are the b-tagging efficiency and the ISR/FSR modeling systematics that account for approximately 80% of the total systematic uncertainty. The NN analysis result is cross-checked with the cut-based method, using additional cuts in order to increase the expected significance of the
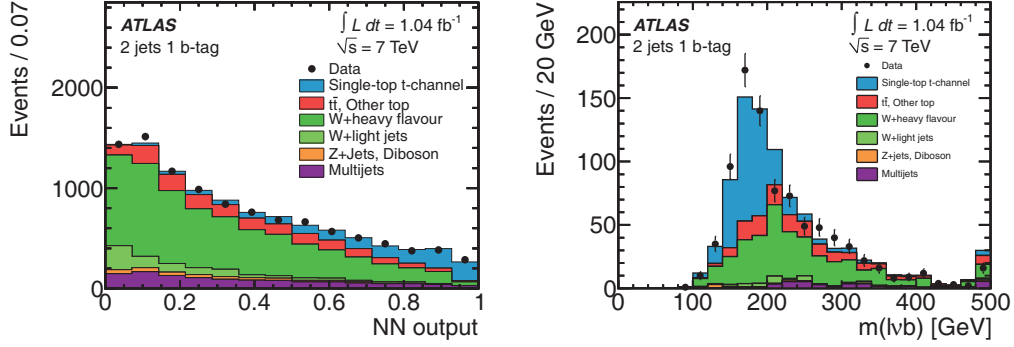
Fig. 3. – Left: the NN output distribution used for extracting the t-channel single top cross section. Right: estimator of the invariant top mass after cut-based method requirements. The signal is normalized to NN fit result (left) and to the observed cross section (right). Source: [8].

t-channel single-top-quark signal. The distribution of the invariant top mass estimator obtained in cut-based method is shown in fig. 3 (right). The CKM matrix element $|V_{tb}|$ is measured to be $|V_{tb}| = 1.13 +0.14 -0.13$ and $|V_{tb}| = 1.03 +0.16 -0.19$ in t- and Wt-channel analyses.

A search for the FCNC has also been performed for the single top production with $\mathcal{L}_{int} = 2.05\,fb^{-1}$ [48]. The search results are consistent with the SM hypothesis and the following 95% CL limits are set: $\sigma(qg \to t) \cdot B(t \to Wb) < 3.9\,pb$ and $B(t \to ug) < 5.7 \cdot 10^{-5}$, $B(t \to cg) < 2.7 \cdot 10^{-4}$.

5. – Summary

The knowledge of top-physics is extended by new and more precise results obtained at ATLAS with the data collected in 2011 at 7 TeV centre-of-mass energy. The results obtained to date are consistent with the SM predictions. It is expected that more data than in 2011 will be collected at 8 TeV center of mass collisions during 2012, hence statistical uncertainty of top quark measurements will be reduced. The systematics uncertainty due to the jet energy scale and generator modeling which are dominant uncertainty sources in many measurements will also be reduced. The latter is expected to decrease notably due to generator tuning and comparisons to the LHC data (*e.g.* [49]). ATLAS will therefore continue to play a key role in top physics efforts.

REFERENCES

[1] ATLAS COLLABORATION, *JINST*, **3** (2008) S08003.
[2] ATLAS COLLABORATION, top group public results webpage: `https://twiki.cern.ch/twiki/bin/view/AtlasPublic/TopPublicResults`.
[3] ATLAS COLLABORATION, ATLAS-CONF-2012-042, `https://cdsweb.cern.ch/record/1435196`.
[4] ATLAS COLLABORATION, ATLAS-CONF-2010-038, `https://cdsweb.cern.ch/record/1277678`.
[5] ATLAS COLLABORATION, *JHEP*, **05** (2012) 059.

[6] ATLAS Collaboration, ATLAS-CONF-2011-121, `http://cdsweb.cern.ch/record/1376413`.
[7] ATLAS Collaboration, ATLAS-CONF-2011-140, `http://cdsweb.cern.ch/record/1385033`.
[8] ATLAS Collaboration, *Phys. Lett. B*, **717** (2012) 330.
[9] ATLAS Collaboration, *Phys. Lett. B*, **716** (2012) 142.
[10] ATLAS Collaboration, ATLAS-CONF-2011-118, `http://cdsweb.cern.ch/record/1376410`.
[11] Cacciari M. *et al.*, *JHEP*, **07** (2003) 001.
[12] ATLAS Collaboration, *Eur. Phys. J. C*, **71** (2011) 1512.
[13] ATLAS Collaboration, *Eur. Phys. J. C*, **72** (2012) 1844.
[14] ATLAS Collaboration, ATLAS-CONF-2011-102, `https://cdsweb.cern.ch/record/1369219`.
[15] Frixione S. *et al.*, *JHEP*, **06** (2002) 029.
[16] Corcella G. *et al.*, *JHEP*, **01** (2001) 010.
[17] Butterworth J. M. *et al.*, *Z. Phys. C*, **72** (1996) 637.
[18] Kerševan B. P. *et al.*, arXiv:hep-ph/0405247.
[19] Sjostrand T. *et al.*, *JHEP*, **05** (2006) 026.
[20] ATLAS Collaboration, ATL-PHYS-PUB-2010-014, `https://cdsweb.cern.ch/record/1303025`.
[21] ATLAS Collaboration, ATLAS-CONF-2010-031, `https://cdsweb.cern.ch/record/1277665`.
[22] Frixione S. *et al.*, *JHEP*, **11** (2007) 070.
[23] Mangano M. L. *et al.*, *JHEP*, **07** (2003) 001.
[24] Gleisberg T. *et al.*, *JHEP*, **02** (2009) 007.
[25] Agostinelli S. *et al.*, *Nucl. Instrum. Methods A*, **506** (2003) 250.
[26] Aliev M. *et al.*, *Comput. Phys. Commun.*, **182** (2011) 1034.
[27] Nadolsky P. M. *et al.*, *Phys. Rev. D*, **78** (2008) 013004.
[28] Kidonakis N., *Phys. Rev. D*, **83** (2011) 091503; **81** (2010) 054028; **82** (2010) 054018.
[29] Martin A. D. *et al.*, *Eur. Phys. J. C*, **63** (2009) 189.
[30] ATLAS Collaboration, *Eur. Phys. J. C*, **72** (2012) 2046.
[31] ATLAS Collaboration, *Phys. Rev. Lett.*, **108** (2012) 212001.
[32] ATLAS Collaboration, *Eur. Phys. J. C*, **72** (2012) 2039.
[33] D0 Collaboration, *Phys. Rev. Lett.*, **100** (2008) 142002; *Phys. Rev. D*, **84** (2011) 112005; CDF Collaboration, *Rev. Lett.*, **101** (2008) 202001; *Phys. Rev. D*, **83** (2011) 112003.
[34] ATLAS Collaboration, *JHEP*, **06** (2012) 088.
[35] ATLAS Collaboration, ATLAS-CONF-2011-141, `http://cdsweb.cern.ch/record/1385517`.
[36] ATLAS Collaboration, ATLAS-CONF-2011-154, `http://cdsweb.cern.ch/record/1398198`.
[37] ATLAS Collaboration, ATLAS-CONF-2011-142, `http://cdsweb.cern.ch/record/1385518`.
[38] ATLAS Collaboration, ATLAS-CONF-2011-153, `http://cdsweb.cern.ch/record/1398197`.
[39] ATLAS Collaboration, *Phys. Rev. D*, **86** (2012) 012007.
[40] ATLAS Collaboration, *Phys. Rev. Lett.*, **108** (2012) 261802.
[41] ATLAS Collaboration, *JHEP*, **04** (2012) 069.
[42] ATLAS Collaboration, *Phys. Rev. Lett.*, **109** (2012) 032001.
[43] ATLAS Collaboration, *Phys. Rev. Lett.*, **108** (2012) 041805.
[44] ATLAS Collaboration, *Phys. Rev. D*, **88** (2012) 032004.
[45] ATLAS Collaboration, *Eur. Phys. J. C*, **72** (2012) 2093.
[46] ATLAS Collaboration, *Phys. Rev. Lett.*, **109** (2012) 081801.
[47] Tait T. M. P. and Yuan C. P., *Phys. Rev. D*, **63** (2000) 014018.
[48] ATLAS Collaboration, *Phys. Lett. B*, **712** (2012) 351.
[49] ATLAS Collaboration, *Eur. Phys. J. C*, **72** (2012) 2043.